hanced pigment excretion again was detectable 5 minutes after illumination began.

These results show that the physiologic response of jaundiced rats to blue light is mediated via the skin surface without involving pineal or visual photoreceptors. As in vision or phytochrome-mediated processes in plants, the photobiologic response is fast even at low light intensities. Pronounced changes in bile composition are observed in minutes, in contrast to the hours of phototherapy required to produce significant changes in plasma bilirubin concentration. Obviously, the plasma bilirubin concentration is not a sensitive or direct measure of the photobiologic response, and its value in studying the mechanism and kinetics of phototherapy is limited.

The mechanism for the enhanced excretion of unconjugated bilirubin during phototherapy is unknown. A current hypothesis cites geometric isomerization (*6*). Bilirubin IXα, which has two *Z*-configuration bridge double bonds (*7*) and requires conjugation for excretion, is thought to be converted by absorption of light to *E-Z* or *E-E* isomers that can be excreted without conjugation. Our observations are compatible with this theory and consistent with immediate formation of a compound in the skin that migrates to the blood, is taken up by the liver, and is rapidly excreted in bile. Although increased pigment excretion is detectable very soon after illumination begins, the response is rather slow compared to the excretion of exogenous anions such as bromosulfophthalein or rose bengal, which appear in bile less than 1 minute after an intravenous pulse injection (*8*). Quite likely, pigment excretion in phototherapy is delayed somewhat because the putative bilirubin isomers or other pigments that are generated photochemically have to pass from extravascular tissues to plasma before they can be cleared and excreted.

Additionally, these studies show that high-pressure liquid chromatography flow-cell detectors, which are readily available, can be used to monitor pigment concentrations in rat bile continuously and directly. This sensitive technique has several advantages over the usual batch-sampling methods and is valuable for studying the hepatic excretion and metabolism of endogenous and exogenous pigments (*8*).

ANTONY F. MCDONAGH
LORI M. RAMONAS
Department of Medicine and
The Liver Center,
University of California,
San Francisco 94143

References and Notes

1. A. K. Brown and J. Showacre, *Phototherapy for Neonatal Hyperbilirubinemia* [U.S. Department of Health, Education, and Welfare Publication No. (NIH) 76-1075, 1977]; R. E. Behrman *et al.*, *J. Pediatr.* **84**, 135 (1974); L. M. Gartner and K.-S. Lee, in *Neonatal-Perinatal Medicine*, R. E. Behrman, Ed. (Mosby, St. Louis, 1977), pp. 394–415.
2. J. D. Ostrow, *J. Clin. Invest.* **50**, 707 (1971).
3. T. P. Vogl, *J. Pediatr.* **85**, 707 (1974).
4. The detector used was a model 153 fixed-wavelength, dual-beam detector made by Altex Scientific Inc., Berkeley, Calif., and fitted with a 470-nm wavelength filter. Further details of this procedure will be published elsewhere (L. M. Ramonas and A. F. McDonagh, in preparation).
5. J. R. Hewitt, R. M. Klein, J. F. Lucey, *Biol. Neonate* **21**, 112 (1972).
6. D. A. Lightner, *Photochem. Photobiol.* **26**, 427 (1977); A. O. Pedersen, F. Schønheyder, R. Brodersen, *Eur. J. Biochem.* **72**, 213 (1977).
7. R. Bonnett, J. E. Davies, M. B. Hursthouse, *Nature (London)* **262**, 326 (1976).
8. L. M. Ramonas and A. F. McDonagh, in preparation.
9. This work was supported by grants (NIAMDD) P50 AM-18520 and AM-18220 from the National Institutes of Health. We thank Leon H. Johnson and Carl Shackleford for advice and assistance.

31 March 1978; revised 30 May 1978

Time-Resolved Resonance Raman Spectroscopy of Hemoglobin Derivatives: Heme Structure Changes in 7 Nanoseconds

Abstract. *Resonance Raman spectra of oxyhemoglobin, deoxyhemoglobin, carboxyhemoglobin, and the corresponding myoglobin derivatives have been obtained with 7-nanosecond laser pulses at 531.8 nanometers. The results suggest that no transient constraint of the heme group by the globin structure occurs on this time scale, and thus establish a temporal sequence for the early events that may participate in the stereochemical trigger mechanism of hemoglobin cooperativity.*

We have recorded the resonance Raman spectra of oxyhemoglobin (O_2Hb), deoxyhemoglobin (deoxy Hb), carboxyhemoglobin (COHb), and the corresponding myoglobin derivatives, using 7-nsec excitation pulses at the second harmonic wavelength (531.8 nm) of an Nd:YAG laser. In the case of COHb, essentially complete photodissociation of CO from the heme iron occurs in the first few hundred picoseconds during which the laser pulse impinges on the sample. Therefore, the observed resonance Raman scattering is predominantly due to photodissociated COHb. Inasmuch as the protein structural relaxations that follow photodissociation of COHb are thought to occur with half-lives of 40 nsec or longer (*1*), the "COHb" spectra that we observe are actually spectra of hemoglobin in which the heme group is deoxy, but the protein remains predominantly in its ligated (oxy) tertiary and quaternary structures. Nevertheless, the time-resolved resonance Raman spectra of photodissociated COHb appear insignificantly different from those of deoxy Hb. The implications of this result for the dynamics and statics of hemoglobin cooperativity are discussed.

The apparatus employed to record the time-resolved resonance Raman spectra will be described in detail elsewhere (*2*). Resonance Raman scattering was excited by repetitive (5 to 20 Hz) pulses from a *Q*-switched frequency-doubled Nd:YAG oscillator (Quanta-Ray DCR-1). This laser is capable of delivering 75 mJ pulses at 531.8 nm; the energy per pulse used in this study was varied between 3 and 27 mJ. The measured pulse width at 531.8 nm was 7 nsec (full width at half-maximum). Raman-scattered light from the sample was collected at $f/1$ using essentially conventional illuminator optics, and focused at $f/7$ into a vidicon spectrograph consisting of a Spex 1870 0.5-m spectrograph with a Princeton Applied Research 1205I detector head in the image plane. This arrangement allowed simultaneous detection of a 345 cm^{-1} segment of the Raman spectrum with peak positions accurate to within 2 cm^{-1}. Spectra were processed by the Princeton Applied Research optical multichannel analyzer console and recorded on an X-Y plotter. Hemoglobin was isolated from human whole blood by a modification of the method of Drabkin (*3*). Resonance Raman spectra were obtained at 25°C in aqueous solution, *p*H 7.0, at a total heme concentration of 0.5 to 1.0 m*M*. Oxyhemoglobin was observed in air-saturated solutions and deoxyhemoglobin was formed by reduction with excess sodium dithionite. Carboxyhemoglobin was formed from the deoxy Hb solution by addition of CO and was observed under 1 atm of CO. Myoglobin was obtained from Sigma (type I, from equine skeletal muscle) and observed under the same conditions as hemoglobin.

The generally accepted model for hemoglobin cooperativity proposes that the "stereochemical trigger" for the change from the ligated (oxy tertiary and R quaternary) to the unligated (deoxy tertiary and T quaternary) protein conformation is the spin-state change of the iron atom on deligation at the axial site *trans* to the proximal histidine (*4, 5*). This spin-state change is accompanied (or followed) by

0036-8075/78/0901-0831$00.50/0

displacement of the iron atom out of the heme plane toward the proximal histidine, and probably by appreciable lengthening of the iron-imidazole bond. The heme structure change is transmitted to the protein tertiary and quaternary structures, effecting the observed cooperativity of ligand binding in the tetrameric protein. The temporal relationships among the events of heme deligation, spin-state change, heme structure change, and protein structure change are of importance in understanding the relationships between heme structure and protein function. Inasmuch as conventional continuous-wave (CW) resonance Raman spectroscopy is a well-established probe for equilibrium heme electronic states and structures (*6*), time-resolved resonance Raman spectroscopy may be expected to provide similar information on heme transients and their temporal behavior.

The available evidence on the dynamics of COHb photolysis (including this work) suggests that the following events occur.

1) $\text{COHb} \xrightarrow[t_{1/2} < 0.5 \text{ psec}]{h\nu,\ \phi \sim 0.5} \text{CO} + \text{Hb}_{4^\circ\text{R}}^{3^\circ\text{Oxy}}$ (*7*)

2) $\text{Hb}_{4^\circ\text{R}}^{3^\circ\text{Oxy}}$ (Fe in plane) $\xrightarrow{t_{1/2} << 7 \text{ nsec}}$ $\text{Hb}_{4^\circ\text{R}}^{3^\circ\text{Oxy}}$ (Fe out of plane) (this work)

3) $\text{Hb}_{4^\circ\text{R}}^{3^\circ\text{Oxy}} \xrightarrow{t_{1/2} = 40\text{–}90 \text{ nsec}} \text{Hb}_{4^\circ\text{R}}^{3^\circ\text{Deoxy}}$ (*1*)

4) $\text{Hb}_{4^\circ\text{R}}^{3^\circ\text{Deoxy}} \xrightarrow{t_{1/2} < 1 \text{ msec}} \text{Hb}_{4^\circ\text{T}}^{3^\circ\text{Deoxy}}$ (*8, 9*)

5) $\text{Hb} + \text{CO (1 atm)} \xrightarrow[<100 \text{ msec}]{\text{complete in}} \text{COHb}$ (*10*)

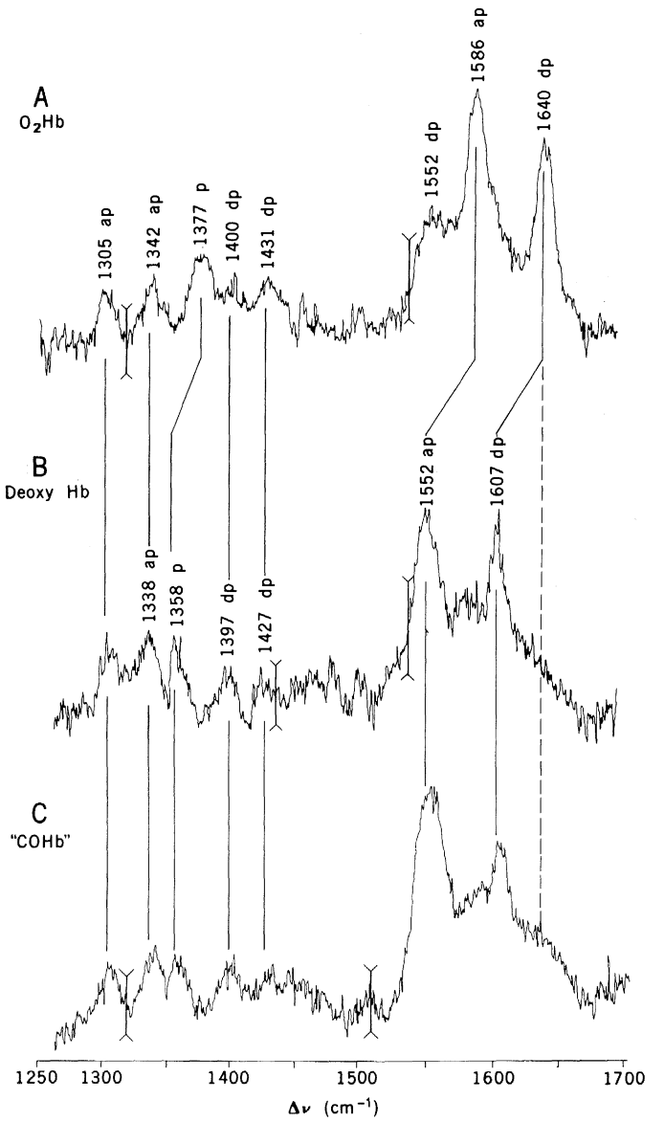

Fig. 1. Time-resolved resonance Raman spectra of (A) oxyhemoglobin, (B) deoxyhemoglobin, and (C) photodissociated carboxyhemoglobin (see text), in the frequency region of the structure-sensitive indicator bands. Abbreviations: *p*, polarized; *dp*, depolarized; and *ap*, anomalously (inversely) polarized. Conditions: excitation, 531.8 nm; pulses, 7 nsec; pulse repetition frequency, 10 Hz; pulse energy, 10 mJ; and accumulation time, 165 seconds. The double-ended arrows in each spectrum denote the points where adjacent vidicon frames were joined to make up complete spectra.

where ϕ is the quantum yield and 3° and 4° refer to the tertiary and quaternary structures of the protein. In a typical experiment, we illuminate the Raman scattering volume of our sample with 7-nsec laser pulses of wavelength 531.8 nm, energy 10 mJ, and repetition rate 10 Hz. Each pulse is sufficiently intense to photodissociate all of the COHb within the scattering volume in approximately 300 psec, which is the time required to deliver a sufficient number of photons to complete reaction 1 above. The remainder of the laser pulse "sees" only the product of reaction 1 or 2 plus any $\text{Hb}_{4^\circ\text{R}}^{3^\circ\text{Deoxy}}$ that has been produced by reaction 3. During our 7-nsec laser pulse, at most 11 percent of the total photodissociated Hb can produce $\text{Hb}_{4^\circ\text{R}}^{3^\circ\text{Deoxy}}$. Our time-resolved resonance Raman spectra of COHb therefore represent approximately 86 percent $\text{Hb}_{4^\circ\text{R}}^{3^\circ\text{Oxy}}$, 10 percent $\text{Hb}_{4^\circ\text{R}}^{3^\circ\text{Deoxy}}$, and 4 percent COHb. Also, since COHb is completely re-formed in less than 0.1 second, 10-Hz laser pulses can be repeated indefinitely to improve the spectral signal-to-noise ratio by signal accumulation.

Figure 1 shows the time-resolved resonance Raman spectra of the structure-sensitive spectral regions (1300 to 1700 cm^{-1}) of O_2Hb, deoxy Hb, and COHb (photodissociated, as noted above). In these experiments, O_2Hb remains ligated because of its relatively low quantum yield of photodissociation. The spectra of O_2Hb and deoxy Hb appear insignificantly different from the respective CW spectra excited at similar laser wavelengths. The three indicator bands that reflect the heme electronic or geometric structure shift from 1377, 1586, and 1640 cm^{-1} in O_2Hb to 1358, 1552, and 1607 cm^{-1} in deoxy Hb, as expected (*6, 11*). The two highest-frequency vibrations are thought to be sensitive primarily to displacement of the iron atom in or out of the heme plane, particularly when the iron atom and the heme are far from coplanar (as in deoxy Hb) (*11–13*).

The spectrum of photodissociated COHb in Fig. 1 is essentially the same as that of deoxy Hb (the same result is obtained with myoglobin). This suggests that the structural relaxations of the heme group following photodissociation of COHb are complete in much less than 7 nsec, despite the evidence that the protein structural relaxations take place in longer times (see reaction 2). Two points are clear from this result: first, the proposed stereochemical trigger for cooperativity in hemoglobin (the heme structure change) is temporally decoupled from the protein reorganizations that it purportedly triggers, and second, the

nonequilibrium globin structure in photodissociated Hb_{4PR}^{20xy} apparently exerts no significant transient constraint on the heme structure (at least on the time scale that we are able to observe). Concerning the second point, it has been clearly demonstrated (*12*) that static globin constraints result in no resonance Raman–detectable distortion of the heme group of carp hemoglobin (which can exist in the T or R protein conformation, independent of the ligation state of its hemes). It was conceivable, however, that such an effect of globin constraint might be observed in an experiment sensitive to the dynamics of the structural reorganizations. Our results indicate that no such dynamic effect occurs.

Our results provide new insight into the possible mechanisms of hemoglobin cooperativity. If the stereochemical trigger hypothesis is correct, then the effects of the heme structure change must initially be stored as strain energy exclusively in the globin structure. This strain must, on a longer time scale, trigger the reorganization of the globin tertiary structure. It is entirely plausible that such a temporal sequence could occur, considering the magnitude of the protein reorganizations involved and the likelihood that the globin represents a "weak spring" compared to the heme (*12–15*). Our results are mute concerning the validity of the stereochemical trigger hypothesis; they are equally consistent with its validity or its failure. If, however, the stereochemical trigger is accepted as valid, then our results support the basic premise of the distributed energy model (*15*) of hemoglobin cooperativity, where the free energy of cooperativity is stored as small strains in the globin structure.

WILLIAM H. WOODRUFF
STUART FARQUHARSON
Department of Chemistry, University of Texas, Austin 78712

References and Notes

1. B. Alpert, R. Banerjee, L. Lindqvist, *Proc. Natl. Acad. Sci. U.S.A.* **71**, 558 (1974).
2. W. H. Woodruff and S. Farquharson, in *New Applications of Lasers in Chemistry*, G. M. Hieftje, Ed. (American Chemical Society, Washington, D.C., in press); *Anal. Chem.*, in press.
3. D. L. Drabkin, *J. Biol. Chem.* **164**, 703 (1966).
4. J. L. Hoard, in *Hemes and Hemoproteins*, B. Chance, R. W. Estabrook, T. Yonetani, Eds. (Academic Press, New York, 1966), pp. 9–24; J. L. Hoard, M. J. Hamor, T. A. Hamor, W. S. Caughey, *J. Am. Chem. Soc.* **87**, 2312 (1965).
5. M. F. Perutz, *Nature (London)* **228**, 726 (1970).
6. T. G. Spiro and T. M. Loehr, in *Advances in Infrared and Raman Spectroscopy*, R. J. H. Clark and R. E. Hester, Eds. (Heyden, London, 1975), vol. 1, chap. 3.
7. C. V. Shank, E. P. Ippen, R. Bersohn, *Science* **193**, 50 (1976).
8. C. A. Sawicki and Q. H. Gibson, *J. Biol. Chem.* **251**, 1533 (1976).
9. F. A. Ferrone and J. J. Hopfield, *Proc. Natl. Acad. Sci. U.S.A.* **73**, 4497 (1976).
10. E. Antonini and M. Brunori, *Hemoglobin and Myoglobin in Their Reactions with Ligands* (North-Holland, Amsterdam, 1971).
11. T. G. Spiro and T. C. Strekas, *J. Am. Chem. Soc.* **96**, 338 (1974).
12. D. M. Scholler and B. M. Hoffman, in *Porphyrin Chemistry*, F. R. Longo, Ed. (Ann Arbor Sciences Publishers, Ann Arbor, Mich., 1978).
13. T. G. Spiro and J. M. Burke, *J. Am. Chem. Soc.* **98**, 5482 (1976).
14. W. H. Woodruff, D. H. Adams, T. G. Spiro, T. Yonetani, *ibid.* **97**, 1695 (1975).
15. J. J. Hopfield, *J. Mol. Biol.* **77**, 207 (1973).
16. Supported by NSF grant CHE77-15220.

4 April 1978; revised 31 May 1978

Allergic Orchitis Lesions Are Adoptively Transferred From Vasoligated Guinea Pigs to Syngeneic Recipients

Abstract. *Histopathology typical of allergic orchitis developed in testes of inbred guinea pigs 16 months after vasoligation. A similar histopathology was found in unoperated testes after unilateral vasoligation. Peritoneal exudate cells from vasoligated guinea pigs transferred identical lesions to syngeneic recipients. The testicular lesions in long-term vasoligated guinea pigs have an immunologic basis.*

Allergic orchitis, an experimental autoimmune disease of the testis, is readily induced in guinea pigs after immunization with testis tissue or testicular extracts in complete Freund's adjuvant (*1*). The disease is characterized by inflammation in the testis and loss of spermatogenic cells; Leydig cells, Sertoli cells, and spermatogonia are not affected (*2*). Vasoligation of man and experimental animals results in the production of antibodies to sperm (*3–7*), and concomitant histopathologic changes in the epididymis and the testis have been described (*4–7*). According to some investigators the morphology of these testicular lesions is similar to those of allergic orchitis (*5, 6*). However, it is difficult to distinguish immunologic lesions from pathologic changes that might result from the vasoligation procedure. In this report, testicular lesions were adoptively transferred by the injection of peritoneal exudate cells from long-term

Table 1. Incidence of testicular and epididymal pathology in strain 13 guinea pigs 16 months after bilateral or sham vasoligation. Under general anesthesia and with aseptic technique, both testes were exteriorized through a low midline abdominal incision. For bilateral vasoligation, the vas were ligated by two silver clips, and a silk ligature was placed between the clips, and the bladder and the vas were cut between the clips. The testes were carefully returned to the scrota, and the abdominal wall was closed in layers. For sham-vasoligation, a silk ligature was loosely tied around, but did not constrict, the vas. Two silver clips were placed on tissues adjacent to the ligature. The testes were carefully returned to the scrota, and the abdominal wall was closed in layers.

Vasoligation	*N*	Histologic findings in testis	Number of animals with epididymal granuloma
Bilateral	4	Multiple macrophagic-invasive lesions with many atrophic seminiferous tubules	1
Bilateral	4	Focal macrophagic-invasive lesions with focal hypospermatogenic tubules	2
Bilateral	10	Normal	4
Sham	5	Normal	0

Table 2. Testicular changes in strain 13 guinea pigs 16 months after unilateral vasoligation. The vasoligation was performed as for bilateral vasoligation (Table 1), while the nonvasoligated testis was untouched.

Guinea pig	Testicular histopathology	
	Vasoligated	Nonvasoligated
1301	Normal	Normal
1302	Normal	Normal
1303	Normal	Normal
1304	Numerous macrophagic-invasive lesions	Several macrophagic-invasive lesions
1307	Numerous macrophagic-invasive lesions	Occasional macrophagic-invasive lesions
1308	Numerous macrophagic-invasive lesions and aspermatogenesis in 50 percent of seminiferous tubules	Numerous macrophagic-invasive lesions and some hypospermatogenic seminiferous tubules

0036-8075/78/0901-0833$00.50/0